Wideband Loop Antenna with Split Ring Resonators for Wireless Medical Telemetry

Zhenzhen Jiang, Zhao Wang, Mark Leach, Eng Gee Lim, Jingchen Wang, Rui Pei and Yi Huang

***Abstract*—This letter presents a wideband flexible loop antenna with split ring resonators (SRRs) for use in wireless medical telemetry. This design covers the entire MedRadio band (401-406 MHz) and four Industrial Scientific Medical ISM bands (433.1–434.8, 868.0–868.8, 902.8–928.0 MHz and 2.4-2.48 GHz). The SRRs improve the loop antenna return loss and reduce the power absorbed inside the human body over the multiband frequency ranges; they also result in increased radiation efficiency, gain and transmission coefficient. A human body model has been used to study and optimise antenna performance in a realistic environment and shows a reduction in specific absorption rate (SAR) when the SRRs are used. Measurements are conducted in a tissue-simulating liquid phantom and show good agreement with the simulations. This novel antenna could be used for a range of implantable applications such as wireless data transmission and wireless power transfer.**

***Index Terms*—Implantable antennas, wideband antennas, split ring resonators (SRRs), biomedical applications.**

I. Introduction

WIRELESS telemetry has become increasingly popular for sensing, monitoring and diagnosis in biomedical applications such as peacemakers, defibrillators and capsule endoscopes [1] - [5], as they can detect inner conditions of the human body and wirelessly transmit associated bio-information in real-time to an external receiver over a link distance of typically a few meters. An essential component for any wireless biomedical communication system is an implantable antenna. Considering the volume and types of potential data that could be obtained from the human body and the fact that these types would differ in relation to factors such as age, gender or other physical conditions, it is of interest to maximise the available bandwidth of such a system and ensure that any detuning that may arise due to variable environmental factors does not affect performance.

In addition, implantable antennas also need to be light weight and low profile to minimise patient impact as well as saving space for other essential system components [6] – [8]. Using high permittivity substrates, fractal structures and shorting pins are some popular techniques in antenna split-ring resonator (CSRR) proposed by Pendry et. al. [13], which possess negative permittivity or negative permeability at a desired frequency have been used for miniaturization [14] [15] [16]. These structures have also been shown to reduce the specific absorption rate (SAR), which is a desired characteristic for implantable antennas [17]. A conformal patch antenna with ground plane loaded CSRR was proposed in [17]. However, this design has a very narrow bandwidth centred at 1.2 GHz. As a result, a flexible implantable antenna that covers multibands of interest, with good radiation performance and robustness are desired to accommodate frequency detuning in a realistic environment and maintain stable operation inside the human body.

In this letter, an implantable loop antenna with SRRs that cover the entire MedRadio band (401-406 MHz) and four ISM bands (433.1-434.8, 868.0-868.8, 902.8-928.0 MHz and 2.4-2.48 GHz) is proposed, which offers the choice of operating at different frequencies across all medical related bands for different functions, such as communication and wireless charging. The antenna is designed on a flexible substrate making it adaptable to multiple applications. This investigation focusses on application in wireless capsule endoscopy, in which, real-time images of the human intestinal tract are wirelessly communicated as a pill type capsule passes through the digestive system. Capsule endoscopes typically consist of a transceiver, camera, LEDs, antennas and batteries [7]. Compared to antennas of planar geometry [18] [19], the antenna is usually designed conformal to the capsules cylindrical shape saving internal space. Use of SRRs leads to improved radiation efficiency and increases realised gain.

The paper is structured as follows: Section II details the selection and design of the implantable antenna. The structure is specified, and other factors considered such as the effect of the necessary biocompatible insulation on performance. In Section III, the antenna radiation properties and SAR are investigated. Measurement setup and results inside a tissue-simulating liquid are presented in Section IV and conclusions are offered in Section V.

NA WITH SRRs

The proposed antenna is designed to work within the human body environment. The design has been produced using CST Microwave Studio 2017. The requirements for this antenna are small size, light weight, wide bandwidth and stable radiation performance. According to [20], compared to other electrical type antennas in the near field, the loop antenna has a smaller electric field and wider operating bandwidth, which allows it to maintain stable performance and good efficiency inside the human body. Therefore, the loop antenna is selected as the fundamental structure in this work.

Manuscript received XXXX, 2019; revised XXXX; accepted XXXX. Date of publication XXXX; date of current version XXXX. This work was supported in part by the XJTLU Research Development Fund under Grant PGRS-13-03-06, Grant RDF-14-03-24, and Grant RDF-14-02-48.

Z. Jiang, Z. Wang, M. Leach, E. G. Lim, J. Wang, and R. Pei are with the Department of Electrical and Electronics Engineering, Xi'an Jiaotong Liverpool University, Suzhou 215123, China (e-mail: Zhenzhen.jiang; zhao.wang; mark.leach; enggee.lim; jingchen.wang; rui.pei@xjtlu.edu.cn).

Y. Huang is with the Department of Electrical Engineering and Electronics, University of Liverpool, Liverpool L69 3BX, U.K. (e-mail:, Yi.Huang@liverpool.ac.uk).

Digital Object Identifier 10.1109/AWPL.201x.xxx

A. Antenna Structure

The proposed loop antenna is designed on RO3010 substrate. The antenna structure is substrate, copper superstrate; the substrate and superstrate are the same material with relative permittivity $\varepsilon_r = 10.2$, loss tangent $\tan\delta = 0.0035$ and thickness 0.6 mm. The copper layer is 0.035 mm thick. SRRs are added at both sides of the loop. The dimensions of the SRR unit cell are optimised to provide maximum antenna matching and radiation efficiency with $S_{11} < -10$ dB for all bands of interest. The overall dimension of the planar antenna is 18 x 18 x 1.235 mm^3 (including superstrate). Fig. 1 shows the main structure and Table I details the optimised geometrical parameters of the proposed antenna. To avoid direct contact between the radiator and body tissues, a biocompatible polyamide layer is added to the capsule surface.

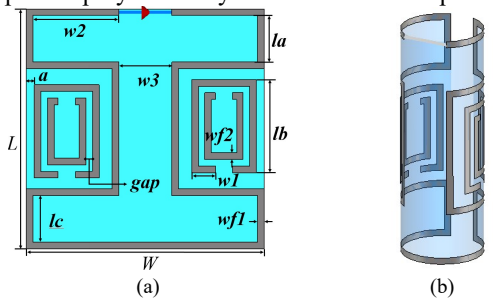

Fig. 1: (a) Geometric design of proposed antenna. (b) Physical layout model of designed antenna.

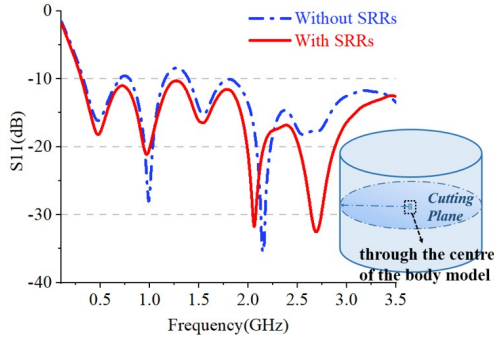

Fig. 2: S_{11} with and without SRRs in the simplified body phantom.

TABLE I

OPTIMISED ANTENNA DIMENSIONS (UNITS: MILLIMETRES)

Parameter	Value	Parameter	Value
L	18	w2	6.5
W	18	w3	4.0
la	3.5	wf1	0.5
lb	7.0	wf2	0.5
lc	3.5	gap	0.5
w1	1.8	a	0.6

Initially to shorten simulation time a simplified homogeneous human body phantom is used based on an elliptical cylinder $120 \times 80 \times 100$ mm^3 with $\varepsilon_r = 56$ and conductivity $\sigma = 0.8$ S/m [6] [21]. The design was later optimised using a more accurate anatomical body model. The simulated reflection coefficient (S_{11}) of the basic loop antenna with and without SRRs in a cylindrical geometry with internal radius 3.2 mm is shown in Fig. 2. The SRRs reduce loop inductance, improving the antenna match. Fig. 3 shows cross-sectional contour plots of the scalar electric near field (E-field) across the centre of the antenna with and without SRRs. The E-field is reduced when the SRRs are employed, leading to a decrease in absorbed power and SAR value (only shown at 403 MHz for brevity but the conclusion is general to other frequencies). Accordingly, the radiated power increases and the radiation efficiency and gain are enhanced.

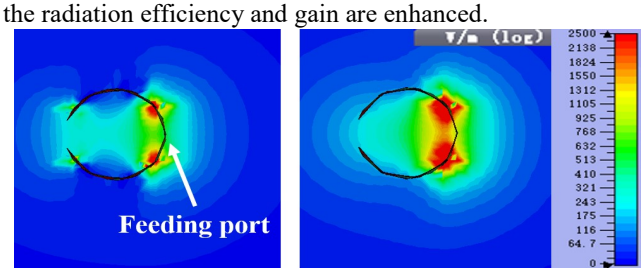

Fig. 3: Top view of the E-field distribution around the proposed antenna in the simplified body phantom at 403 MHz: (a) with SRRs, (b) without SRRs.

B. Effect of Internal Batteries

A conformal antenna on the outer wall of a capsule endoscope saves space for other essential components inside the shell and offers better performance than an antenna inside the capsule [22] [23]. The main solid component of the inner structure is the battery which may influence antenna performance [24]. To investigate the impact of locating a battery inside the capsule surface, a perfect electric conductor is added to the model representing the battery. Simulated S_{11} results with and without a battery are shown in Fig. 4, for different battery sizes and locations. Inclusion of a battery is seen to give rise to a frequency shift. The lower resonant frequencies are shifted from 477 MHz and 0.96 GHz to 577 MHz and 1.28 GHz respectively and the resonant frequency at 2.5 GHz is upshifted by 150 MHz. The operating bandwidth remains almost the same covering all frequency bands of interest despite the frequency shifts.

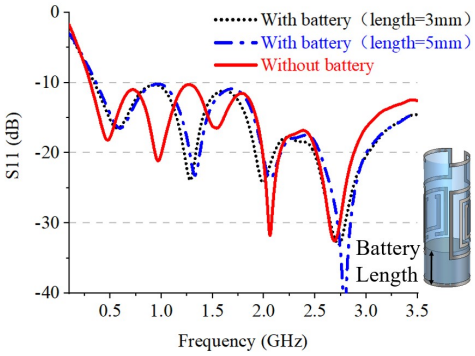

Fig. 4: Simulated S_{11} with internal batteries of different heights.

C. Effect of Biocompatible Insulation

In real implantation cases, the surface of the device is required to be biocompatible. The encapsulation layer reduces the conducting influence of the human body and coupling between the antenna and the surrounding tissue [25]. The proposed antenna is designed on RO3010 substrate which is not biocompatible, therefore the outer surface of the antenna is covered with a thin layer of a low-loss biocompatible polyamide ($\varepsilon_r = 3.5$, $\tan\delta = 0.004$). The effects of different coating thicknesses are demonstrated in Fig. 5, which shows

that frequency shifts due to the coating material increase with coating thickness. Optimisation of S_{11}, leads to a polyamide thickness of 0.017 mm. Alternatively, biocompatible materials could be used for the antenna design [26], replacing the substrate and copper with Al_2O_3 ($\varepsilon_r = 9.8$, $\tan\delta = 0.008$) and silver palladium (Ag/Pd) respectively. Simulation results show that in comparison the resonant frequencies are shifted upwards approximately 40-55 MHz with the antenna covering all bands of interest. However, the RO3010 substrate remains the preferred choice due to the relative ease of manufacture and costs.

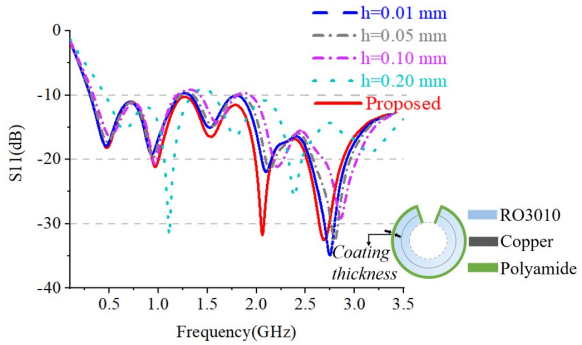

Fig. 5: Effects on S_{11} with different thicknesses of the coating material.

D. Effect of Different Human Tissues

Different from an in-body antenna with a specific implant location, a capsule antenna will travel through the human body, as a result, the influences of different body tissues such as stomach, colon and small intestine should be examined [27]. Fig. 6 illustrates the resultant S_{11} with the same body model shown in Fig. 2 and structure from Fig. 5 but for different body tissues. The resonant frequencies for both the stomach and the small intestine are almost the same as their relative permittivities are close. However, there is a slight upshift in S_{11} for the colon, which has a significantly smaller relative permittivity.

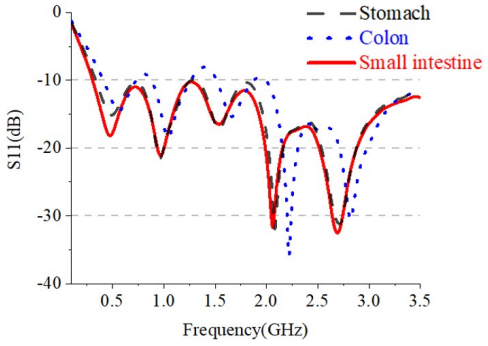

Fig. 6: Effects on S_{11} with different biological tissues.

The proposed antenna has also been evaluated using the same elliptical cylinder shape body model but with muscle equivalent properties (e.g. $\varepsilon_r = 59.2$, 51.9, and $\sigma = 0.77$, 1.74 S/m at 403 MHz and 2.45 GHz, respectively) for comparison with simulation on the arm of the anatomical body model. Corresponding results for S_{11} are plotted in Fig. 7. The radiation pattern in Fig. 9 (b) shows that the proposed antenna provides desirable performance on the arm which suggests muscle is also suitable operating environment.

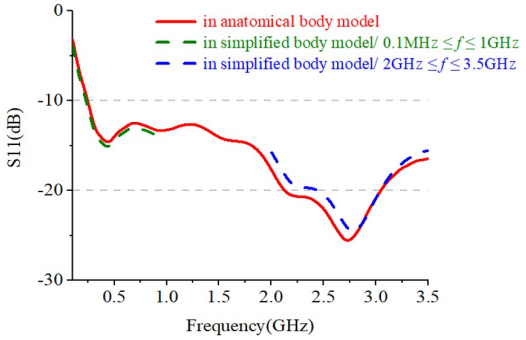

Fig. 7: Simulated S_{11} when putting the antenna on human arm.

III. Radiation Efficiencies and SAR Value

Two-dimensional (2-D) realised gain patterns of the proposed antenna at 403 MHz in the simplified body model (small intestine) and at 2.45 GHz in the anatomical body model (on the arm) are given in Fig. 8 and Fig. 9 respectively (only 2 selected for brevity). The anatomical body model, Gustave from the CST Voxel family is used, (male, height 176 cm, weight 69 kg). The model provides a more accurate simulation environment, allowing SAR values to be obtained.

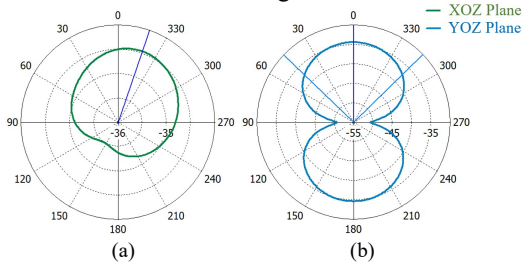

Fig. 8: Simulated 2-D realised gain patterns of proposed implantable antenna at 403 MHz in the simplified body model on: (a) XOZ plane (b)YOZ plane.

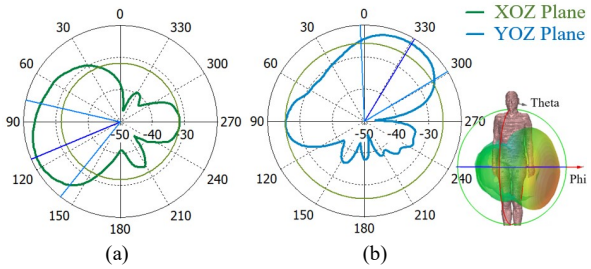

Fig. 9: Simulated 2-D realised gain patterns at 2.45 GHz on the arm in the anatomical body model on: (a) XOZ plane (b)YOZ plane.

Radiation efficiency and realized gain for the antenna with and without SRRs are summarised in Table II. The SRRs improve both parameters across the spectrum. In IEEE standards, the simulated maximum 1 g average SAR value for a transmitter are 216 and 203 W/kg at 403 MHz and 2.45 GHz respectively at an input power of 1 W. Use of SRRs here decreases the SAR by 88 and 62 W/kg at those frequencies respectively, allowing increased transmit powers of 7.41 and 7.88 mW (8.70 and 8.97 dBm) respectively, with SAR limits of 1.6 W/kg [28] [29]. The asymmetric body model, means antenna performance is location dependent. The radiation efficiency and realized gain compared with other works are shown in Table III and an SRR/CSRR functionality comparison to other work is shown in Table IV.

TABLE II

SIMULATED RADIATION EFFICIENCY AND REALISED GAIN WITH AND WITHOUT SRRS

f(MHz)	Radiation Efficiency (%)		Realised Gain (dBi)		Max 1g-avg SAR (W/kg)
	With SRRs	No SRRs	With SRRs	No SRRs	With SRRs
403	0.025	0.023	-34.3	-35.7	216
433	0.077	0.033	-30.6	-33.9	213
868	0.248	0.116	-26.6	-27.6	211
915	0.264	0.190	-26.0	-28.0	205
2450	0.414	0.284	-18.4	-19.1	203

TABLE III

Comparisons of the Proposed Antenna with Other Work

Ref.	f(MHz)	Size (L x R) mm^2	Port No.	Realised Gain (dBi)	Max 1g-avg SAR (W/kg)
[6]	284~825	17 x 3	1	-31.5 (at 403)	913 (at 403)
[30]	2290~2530	15 x 5	1	-44.5 (at 2450)	368.7 (at 2450)
[31]	321~532, (MIS)	17.2 x 5	1	-30.5	72 (over 10g)
	2150~2740 (ISM)			-22.2	48.8 (over 10g)
[32]	296~589	15 x 4.6	2	-33.6 (at 434)	340.6 at port 1 322.3 at port 2 (at 434)
This work	307~3500	18 x 3	1	See TABLE II	

TABLE IV

Comparisons of the Proposed Antenna with Other Metamaterial Work

Ref.	f(MHz)	Type	Function of metamaterial unit (s)
[17]	1200	CSRR	Miniaturise size
[33]	2400~2480	CSRR	Miniaturise size
[34]	402~455, 2400~2480	SRR	Miniaturise size & obtain a new resonance frequency by coupling to a spiral
This work	307~3500	SRR	Reduce E-field & power loss & enhance radiation efficiency

IV. MEASUREMENT SETUP AND RESULTS

The fabricated antenna is shown in Fig. 10(a). It was measured using a homogeneous mixture method proposed in [35] using a calibrated vector network analyser (VNA) port with a 50 Ω RF cable. The tissue-simulating liquid recipes at 403 MHz and 2.45 GHz are summarised in TABLE V. The measurement setup is shown in Fig. 10(b), where the antenna is placed at the centre of a plastic container filled with the mixture. Reflection coefficient results from the VNA are shown in Fig. 11. The blue line represents S_{11} using the liquid phantom recipe at 403 MHz; the green line shows S_{11} with the 2.45 GHz liquid recipe. In comparison to the simulated values the resonant frequencies shift and some discrepancies are seen while both the simulated and measured results are well below -10 dB and in good agreement at all frequencies of interest. Frequency shifting may be caused by the air gap between the superstrate and antenna, fabrication errors or connection issues.

TABLE V

RECIPES FOR THE TISSUE-SIMULATING LIQUIDS

f (MHz)	Sugar	NaCl	De-ionized water	HEC	Diacetin and Glycol	Triton X-100
403	45.17%	2.98%	51.3%	0.5%	0.05%	--
2450	--	--	58.2%	--	5.1%	36.7%

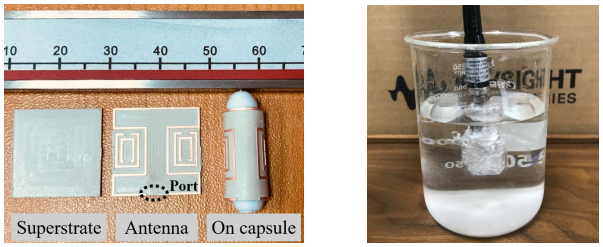

(a) (b)

Fig. 10: (a) Photograph of the fabricated superstrate and antenna (b) Measurement of the proposed antenna in the tissue-simulating liquid.

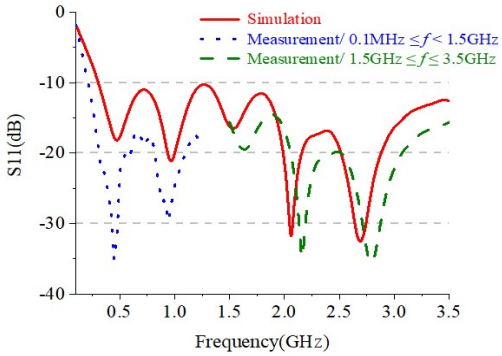

Fig. 11: Measured and simulated S_{11} of the proposed antenna.

V. CONCLUSION

In this letter, an ultra-wideband flexible loop antenna with SRRs has been proposed, designed, fabricated and tested for wireless medical telemetry. It was simulated and measured in both a homogeneous tissue phantom and the Gustave human body model showing acceptable performance. The proposed antenna works over the full MedRadio band and four ISM bands making it suitable for use in low power or passive implant systems. Two SRRs are loaded on the radiator and lead to improved matching and increased radiation efficiency. The influence of capsule dimension, internal batteries and biocompatible insulation on antenna performance is acceptable in terms of band requirements making this a good candidate for implantable applications.

ACKNOWLEDGMENT

Authors would like to thank CST AG for providing the CST STUDIO SUITE Electromagnetic Simulation Software package under the China Key University Promotion Program and the Municipal Key Lab for Wireless Broadband Access Technologies in the Department of Electrical Engineering, Xi'an Jiaotong Liverpool Univ, for research facilities.

REFERENCES

[1] D. Nikolayev, M, Zhadobo, L. Le Coq, P. Karban, and R. Sauleau, "Robust ultraminiature capsule antenna for ingestible and implantable applications," *IEEE Trans. Antennas Propag.,* vol. 65, no. 11, pp. 6107–6119, Nov. 2017.

[2] R. S. Alrawashdeh, Y. Huang, M. Kod, and A. Sajak, "A broadband flexible implantable loop antenna with complementary split ring resonators," *IEEE Antennas Wireless Propag. Lett.*, vol. 14, pp. 1503–1509, Feb. 2015.

[3] G. Ciuti, A. Menciassi, and P. Dario, "Capsule endoscopy: From current achievements to open challenges," *IEEE Rev. Biomed. Eng.*, vol. 4, pp. 59–72, 2011.

[4] A. Kiourti and K. S. Nikita, "Miniature scalp-implantable antennas for telemetry in the MICS and ism bands: Design, safety considerations and link budget analysis," *IEEE Trans. Antennas Propag.*, vol. 60, no. 8, pp. 3568–3575, Aug. 2012.

[5] A. Kiourti, K. A. Psathas, and K. S. Nikita, "Implantable and ingestible medical devices with wireless telemetry functionalities: A review of current status and challenges," *Bioelectromagnetics*, vol. 35, no. 1, pp. 1–15, Jan. 2014.

[6] J. Wang, M. Leach, E. Lim, Z. Wang, R. Pei and Y. Huang, "An Implantable and Conformal Antenna for Wireless Capsule Endoscopy," *IEEE Antennas Wireless Propag. Lett.*, vol. 17, pp. 1153–1157, May. 2018.

[7] W. A. Qureshi, "Current and future applications of the capsule camera," *Nature Rev. Drug Discovery,* vol. 3, pp. 447–450, May 2004.

[8] W. Lei, H. Chu, and Y.-X. Guo, "Design of a circularly polarized ground radiation antenna for biomedical applications," *IEEE Trans. Antennas Propag.,* vol. 64, no. 6, pp. 2535–2540, Jun. 2016.

[9] K. Asimina, and S. N. Konstantina, "A review of implantable patch antennas for biomedical telemetry: challenges and solutions," *IEEE Antennas and Propagation Magazine*, vol. 54, no. 3, pp. 210-228, 2012.

[10] A. Sondas, and M. Ucar, "An implantable microstrip antenna design for biomedical telemetry", *International Conference on Electronics, Computer and Computation (ICECCO) 2013*, pp. 1595-1598, 2013.

[11] C. L. Yang, C. L. Tsai, and S. H. Chen, "Implantable high-gain dental antennas for minimally invasive biomedical devices," *IEEE Trans. Antennas Propag.*, vol. 61, no. 5, pp. 2380–2387, May. 2013.

[12] H. Li, Y. X. Guo, C. Liu, S. Xiao, and L. Li, "A miniature-implantable antenna for Medradio-band biomedical telemetry," I*EEE Antennas Wireless Propag. Lett.*, vol. 14, pp. 1176–1179, Jan. 2015.

[13] C. Caloz, and T. Itoh, Electromagnetic Metamaterials: Transmission Line Theory and Microwave Applications: The Engineering approach. *A John Wiley Sons Inc.*, 2005.

[14] X. Cheng, D. E. C. Kim, and Y. Yoon, "A compact omnidirectional selfpackaged patch antenna with complementary split-ring resonator loading for wireless endoscope applications," *IEEE Antennas Wireless Propag. Lett.*, vol. 10, pp. 1532–1535, 2011.

[15] J. D. Baena et al., "Equivalent-circuit models for split-ring resonators and complementary split-ring resonators coupled to planar transmission lines," *IEEE Trans. Microw. Theory Techn.*, vol. 53, no. 4, pp. 1451–1461, Apr. 2005.

[16] S. Ma, L. Sydanheimo, L. Ukkonen and T. Bjorninen, "Split-Ring Resonator Antenna System With Cortical Implant and Head-Worn Parts for Effective Far-Field Implant Communications," *IEEE Antennas Wireless Propag. Lett.*, vol. 17, no. 4, pp. 710-713, April 2018.

[17] S. M. Asif et al., "Design and in vivo test of a batteryless and fully wireless implantable asynchronous pacing system," *IEEE Trans. Biomedl Eng.*, vol. 63, pp. 1070–1081, Sept. 2016.

[18] C. Liu, Y. Guo, H. Sun and S. Xiao, "Design and safety considerations of an implantable rectenna for far-field wireless power transfer," *IEEE Trans. Antennas Propag.,* vol. 62, no. 11, pp. 5798–5806, Nov. 2014.

[19] F. Huang, C. Lee, C. Chang, L. Chen, T. Yo and C. Luo, "Rectenna application of miniaturized implantable antenna design for triple-band biotelemetry communication," *IEEE Trans. Antennas Propag.,* vol.59, no. 7, pp. 2646–2653, July. 2011.

[20] F. Merli, "Implantable antennas for biomedical applications," Ph.D. dissertation, Department of Electrical Engineering, EPFL Univ., Lausanne, Switzerland, 2011.

[21] C. Gabriel, "Compilation of the dielectric properties of body tissues at RF and microwave frequencies," Brooks Air Force Base, San Antonio, TX, USA, Tech. Rep. AL/OE-TR-1996-0037, 1996.

[22] R. S. Alrawashdeh, Y. Huang, and P. Cao, "Flexible meandered loop antenna for implants in MedRadio and ISM bands," *Electron. Lett.*, vol. 49, no. 24, pp. 1515–1517, Dec. 2013.

[23] Z. Duan and L. Xu, "Dual-ban implantable antenna with circular polarization property for ingestible capsule application," *Electron. Lett.,* vol. 53, no. 16, pp. 1090–1092, Aug. 2017.

[24] Z. Bao, Y. X. Guo, and R. Mittra, "An ultrwideband conformal capsule antenna with stable impedance matching," *IEEE Trans. Antennas Propag.*, vol. 65, no. 10, pp. 5086–5094, Oct. 2017.

[25] F. Merli, B. Fuchs, J. R. Rosig, A. K. Skrivervik, "The effect of insulating layers on the performance of implanted antennas", *IEEE Trans. Antennas Propag.*, vol. 59, no. 1, pp. 21-31, Jan. 2011.

[26] P. Soontornpipit, C. M. Furse, Y. C. Chung, "Design of implantable microstrip antennas for communication with medical implants", *IEEE Trans. Microw. Theory Tech.*, vol. 52, no. 8, pp. 1944-1951, Aug. 2004.

[27] "Calculation of the dielectric properties of boy tissues," Institute for Applied Physics, Italian National Research Council, http://niremf.ifac.cnr.it/tissprop/.

[28] C. Schmidt et al., "Broadband UHF implanted 3-D conformal antenna design and characterization for in-off body wireless links," *IEEE Trans. Antennas Propag.*, vol. 62, no. 3, pp. 1433–1444, Mar. 2014.

[29] *IEEE Standard for Safety Levels with respect to Human Exposure to Radio Frequency Electromagnetic Fields, 3KHz to 300 GHz,* IEEE Standard C95. 1-2005, 2005.

[30] R. Li, Y. X. Guo and G. Du, "A Conformal Circularly Polarized Antenna for Wireless Capsule Endoscope Systems," *IEEE Trans. Antennas Propag.*, vol. 66, no. 4, pp. 2119–2124, April. 2018.

[31] R. Duan, Y. X. Guo, M.Je and D. L. Kwong, "Design and in Vitro Test of a Differentially Fed Dual-Band Implantable Antenna Operating at MICS and ISM Bands," *IEEE Trans. Antennas Propag.*, vol. 62, no. 5, pp. 2430–2439, May. 2014.

[32] W. Lei and Y. X. Guo, "Design of a Dual-Polarized Wideband Conformal Loop Antenna for Capsule Endoscopy Systems," *IEEE Trans. Antennas Propag.,* vol. 66, no. 11, pp. 5706–5715, Nov. 2018.

[33] X. Liu, Z. Wu, Y. Fan and E. M. Tentzeris, "A Miniaturized CSRR Loaded Wide-Beamwidth Circularly Polarized Implantable Antenna for Subcutaneous Real-Time Glucose Monitoring," *IEEE Antennas Wireless Propag. Lett.*, vol. 16, pp. 577-580, 2017.

[34] C. J. Sa´nchez-Ferna´ndez, O´ scar Quevedo-Teruel, J. Requena-Carri´on, L. Incl´an-S´anchez, Eva Rajo-Iglesias, Malcolm Ng Mou Kehn , "Dual- band implantable antenna based on short-curcuited SRR" *in Proc. EuCAP*, Barcelona, Spain, 2010, pp.1-4.

[35] T. Yilmaz, T. Karacolak, and E. Topsakal, "Characterization and testing of a skin mimicking material for implantable antennas operation at ISM band (2.4 GHz–2.48 GHz)," *IEEE Antennas Wireless Propag. Lett.*, vol. 7, pp. 418-420, 2008.